Supporting information

A 3D Lithiophilic ZIF-8@rGO Free-standing Scaffold with Dendrite-free Behavior Enabling High-performance Li Metal Batteries

Qi Liu[a], Rilei Wang[a], Zhenfang Liu[a], Xianshu Wang[d*], Cuiping Han[c], Hongbo Liu[a*], Baohua Li[b*]

[a] *College of Materials Science and Engineering, Hunan University, Changsha, 410082, Hunan, China*

[b]*Shenzhen Key Laboratory of Power Battery Safety and Shenzhen Geim Graphene Center, Tsinghua Shenzhen International Graduate School, Tsinghua University, Shenzhen, 518055, China.*

[c] *Faculty of Materials Science and Engineering, Institute of Technology for Carbon Neutrality, Shenzhen Institute of Advanced Technology, Chinese Academy of Sciences (CAS), Shenzhen, Guangdong, 518055 China*

[d] *National and Local Joint Engineering Laboratory for Lithium-ion Batteries and Materials Preparation Technology, Key Laboratory of Advanced Battery Materials of Yunnan Province, Faculty of Metallurgical and Energy Engineering, Kunming University of Science and Technology, Kunming, 650093, People's Republic of China*

Corresponding Email: xswang2016@m.scnu.edu.cn;
hndxlhb@163.com;
libh@mail.sz.tsinghua.edu.cn

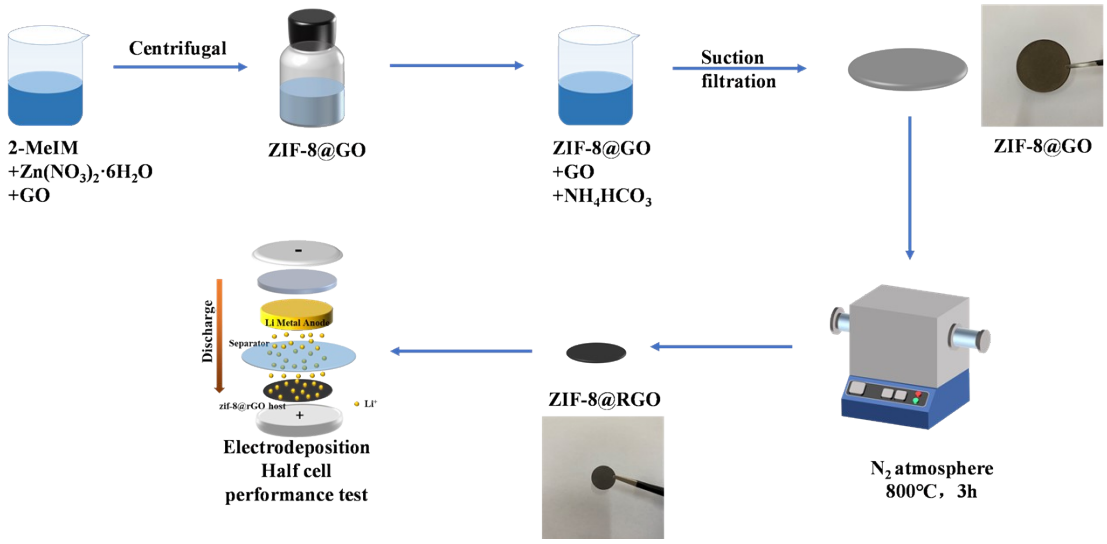

Figure S1. Schematic illustration of the synthesis procedure of ZIF-8@RGO.

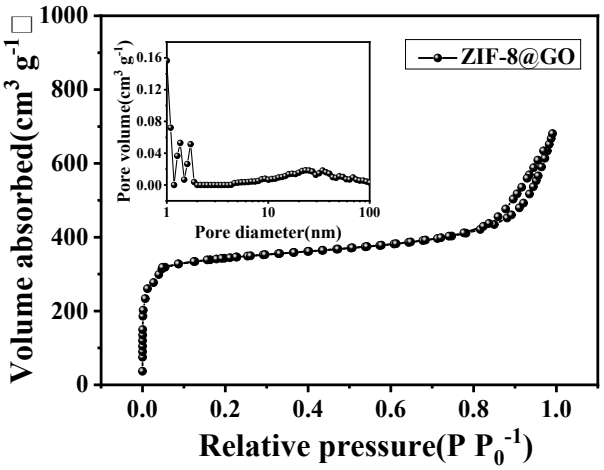

Figure S2. Nitrogen adsorption-desorption isotherms of ZIF-8@GO, and insert is the corresponding pore size distributions calculated from the non-local density functional theory model.

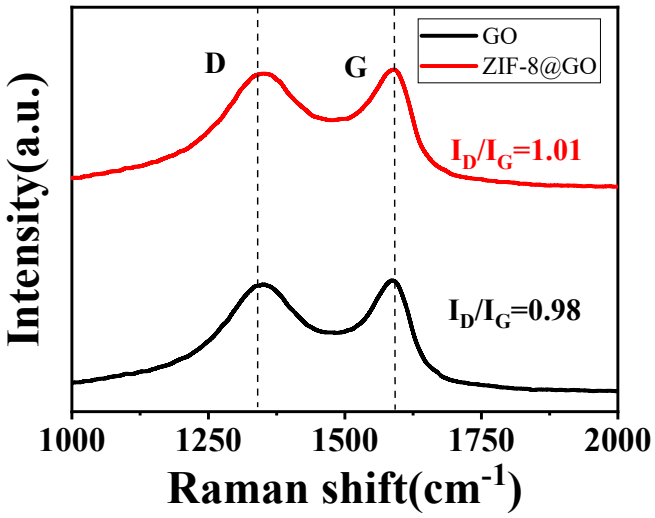

Figure S3. Raman spectra of GO and ZIF-8@GO.

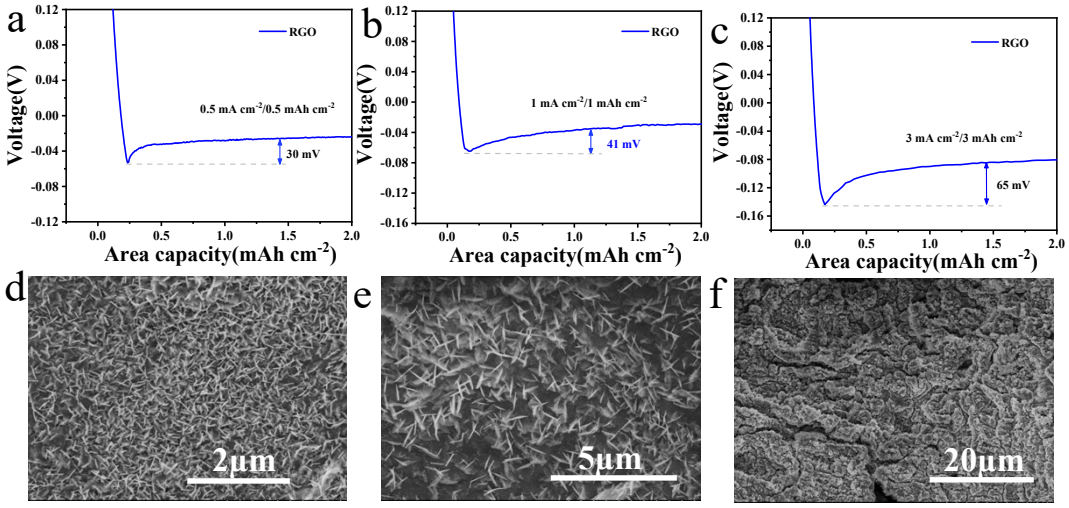

Figure S4. The discharge profiles (a-c) and surface SEM morphologies (d-f) of Li plating on RGO after plating (a, d) 0.5 mA cm^{-2} /0.5 mAh cm^{-2}, (b, e) 1 mA cm^{-2} /1 mAh cm^{-2}, (c, f) 3 mA cm^{-2} /3 mAh cm^{-2}.

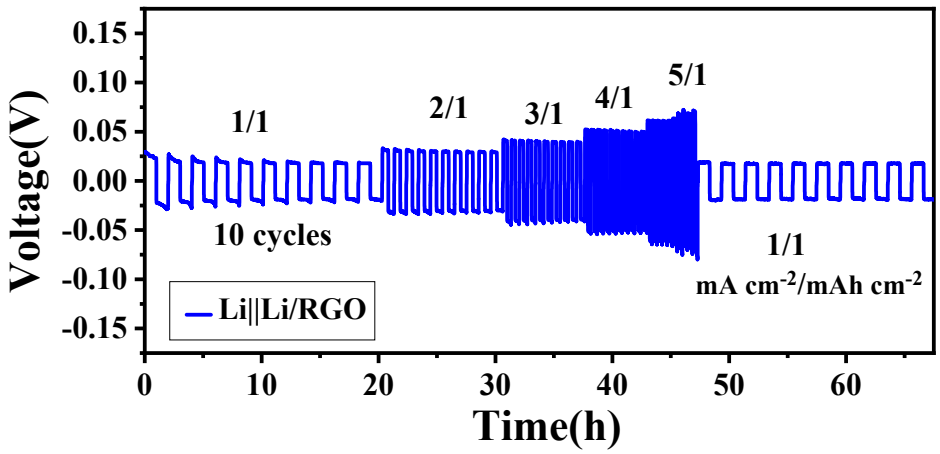

Figure S5. Comparison of the rate performance of RGO in symmetric cells

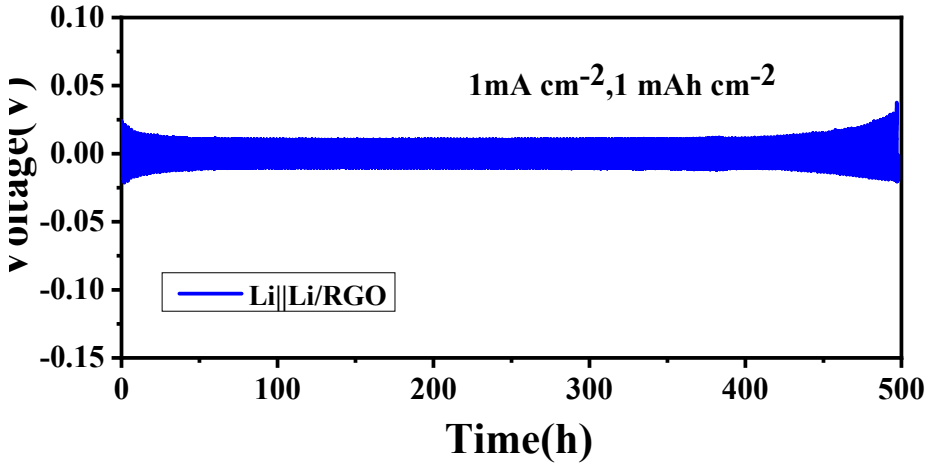

Figure S6. The cycling stability of RGO in symmetric cells at 1 mA cm^{-2} for 1 mAh cm^{-2}.

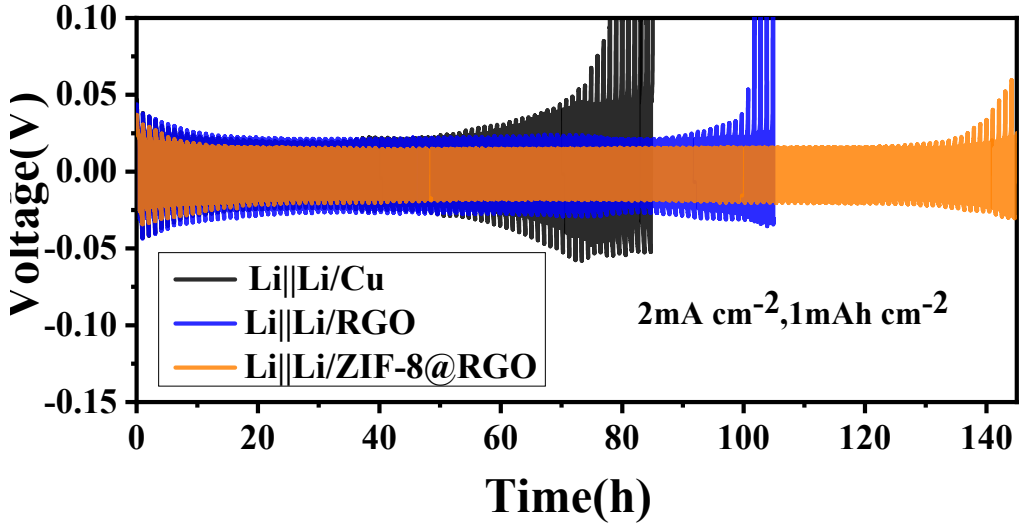

Figure S7. The cycling stability of Cu, RGO and ZIF-8@RGO in symmetric cells at 2 mA cm^{-2} for 1 mAh cm^{-2}.

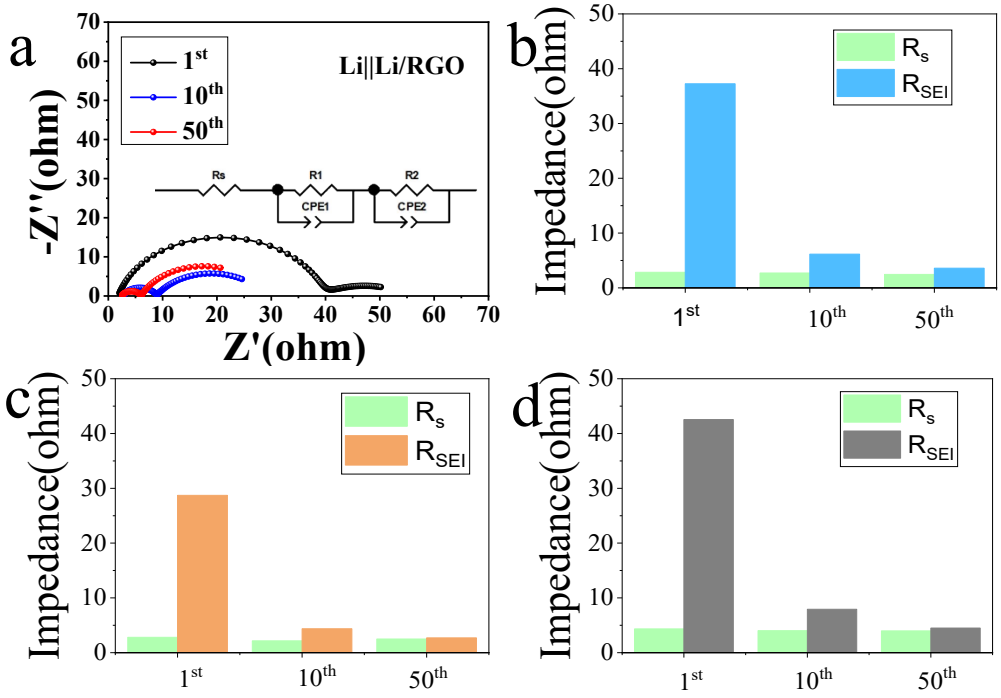

Figure S8. a) EIS spectra of RGO at different cycles at 1 mA cm^{-2} for 1 mAh cm^{-2}, Inset: the fitting equivalent circuit model. The corresponding fitting results of b) bare Cu, c) ZIF-8@RGO and d) RGO in Li|Li symmetric cells after different cycles. Rs and RSEI represent the cell bulk impedance and interfacial impedance, respectively.

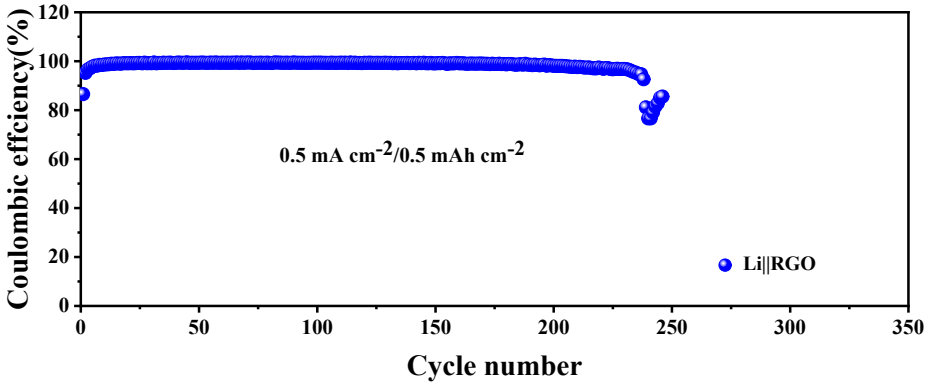

Figure S9. CE of the Li plating/stripping on RGO with a capacity of 0.5 mAh cm^{-2} at 0.5 mA cm^{-2}.

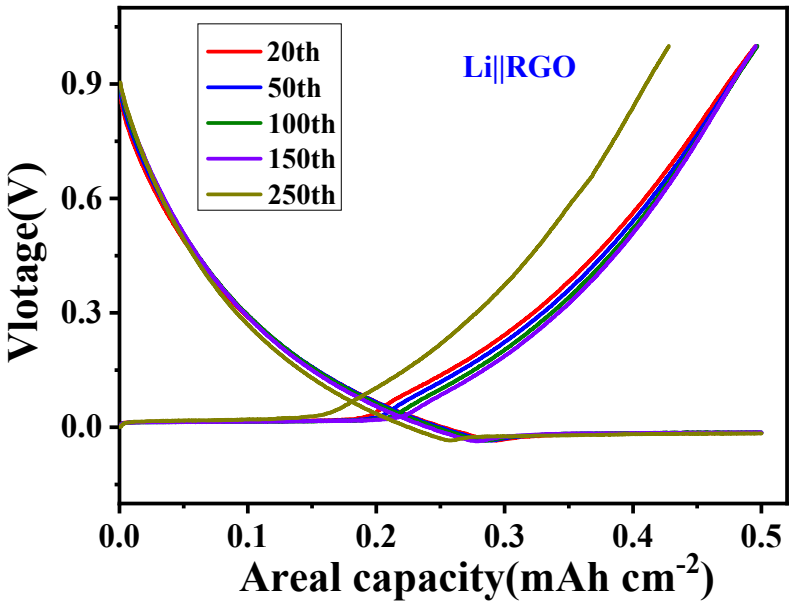

Figure S10. The corresponding voltage profiles of Li plating/stripping on RGO with a capacity of 0.5 mAh cm^{-2} at 0.5 mA cm^{-2}.

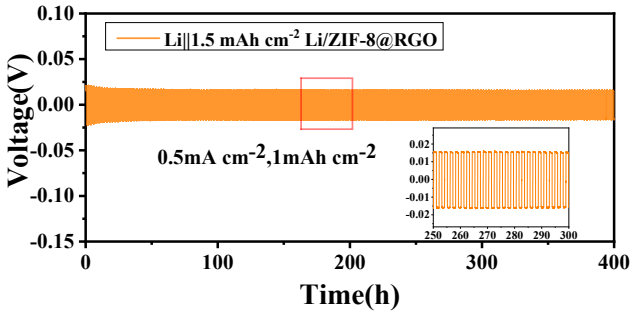

Figure S11. the cycling stability of 1.5 mAh cm^{-2} ZIF-8@RGO in symmetric cells at 0.5 mA cm^{-2} for 1 mAh cm^{-2}.

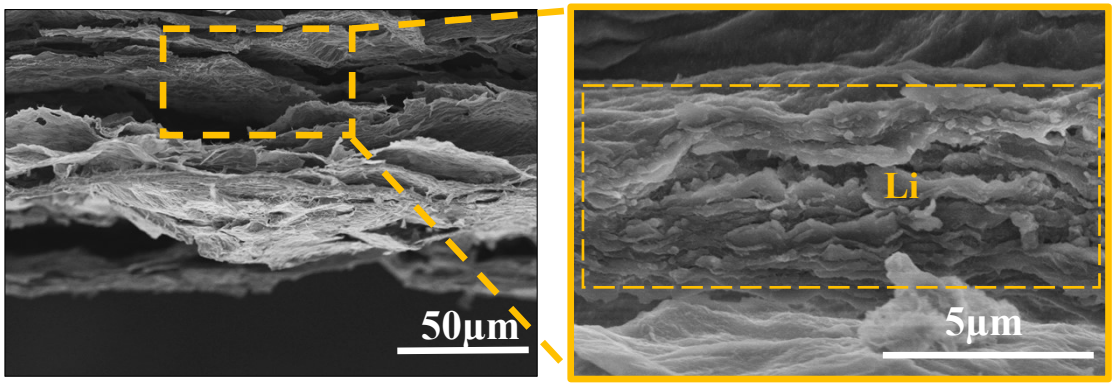

Figure S12. Enlarged cross-sectional SEM images of ZIF-8@RGO after 50 cycles at 0.5 mA cm^{-2} for 0.5 mAh cm^{-2}.

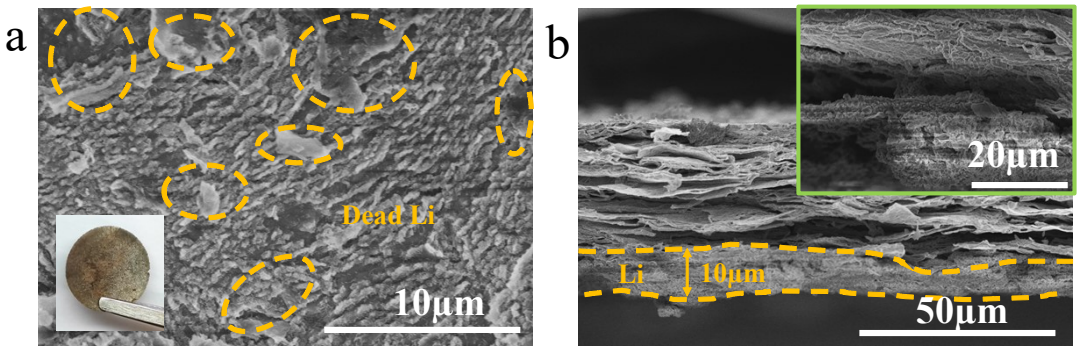

Figure S13. a) Surface and b) Corresponding cross-sectional images of RGO after 50 cycles at 0.5 mA cm^{-2} for 0.5 mAh cm^{-2}. Inserts: optical morphology (Left) and enlarged cross-sectional morphology (Right).

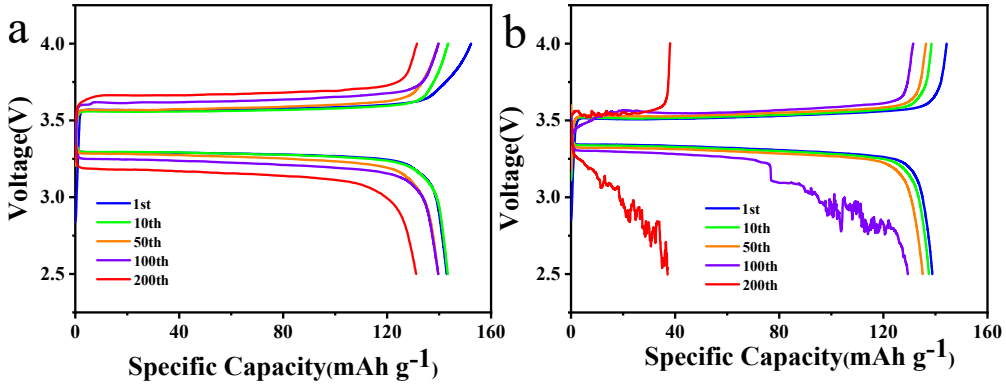

Figure S14. The corresponding charge/discharge profiles after different cycles in full cells with a) ZIF-8@RGO and b) bare Cu as anode at 0.5 C, respectively.

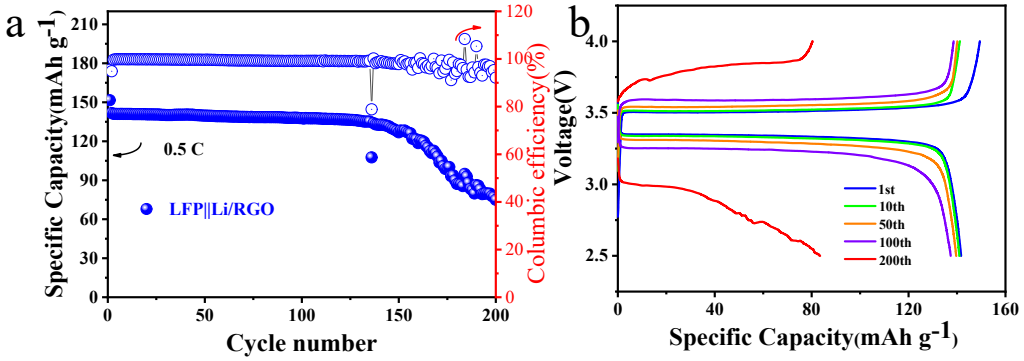

Figure S15. a) Cycling performances and b) corresponding charge/discharge profiles after different cycles of the full cells with RGO as anodes at 0.5 C coupled with LFP cathode.

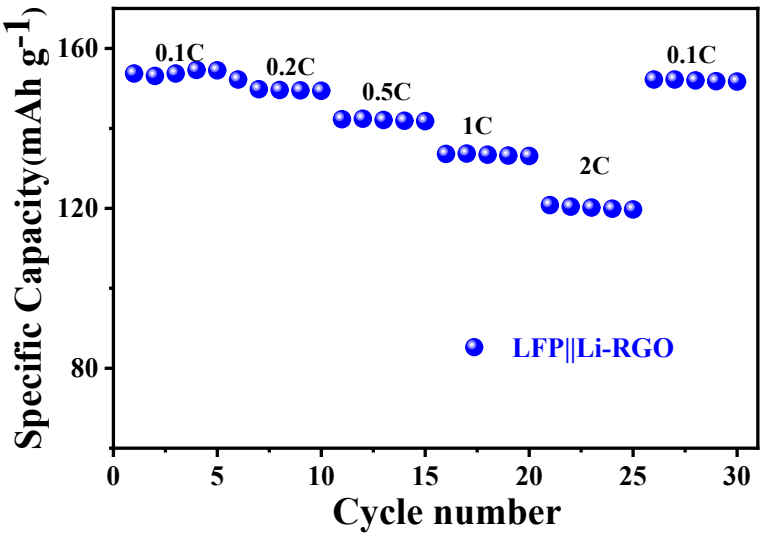

Figure S16. Rare capabilities of the full cells with RGO as anodes at various rates coupled with LFP cathode.

Table S1 Statistical table of element content based on XPS

Sample	C(at%)	O(at%)	N(at%)	Zn(at%)
RGO	90.88	5.4	3.72	/
ZIF-8@RGO	91.18	5.42	3.16	0.24

Table S2 Performance comparisons of different anode electrodes coupled with $LiFePO_4$ cathodes

Electrode	Loading of cathode (mg/cm^{-2})	Rate(C)	Cycling Performance	Ref
VAG@Li	14.10	0.5 (1C=2.1 mA cm^{-2})	A capacity retention of 90.8% over 270 cycles	[1]
CNF-TiN@Li	5.0	1C (1C=0.85 mA cm^{-2}	A higher capacity of 122.4 mAh g^{-1} over 250 cycles	[2]
CNT@Li	14.3	0.4C(1C=2.44 mA cm^{-2})	A capacity retention of 92.6% over 150 cycles	[3]
Zn@NC@CC	13.5	1C(1C=2.295 mA cm^{-2})	A high reversible capacity of 109.3 mA h g^{-1} over 160 cycles	[4]
ZIF-8@RGO@Li	4	0.5C (1C=0.68 mA cm^{-2})	A capacity retention ratio of ~92.87%) with a highest discharge capacity of ~131.6 mAh g^{-1} after 200 cycles	Our work

Reference

1. K. Lin, X. Xu, X. Qin, S. Wang, C. Han, H. Geng, X. Li, F. Kang, G. Chen and B. Li, *Carbon*, 2021, **185**, 152-160.
2. K. Lin, X. Qin, M. Liu, X. Xu, G. Liang, J. Wu, F. Kang, G. Chen and B. Li, *Adv Func Mater* 2019, **29**, 1903229-1903340.
3. Z. Sun, S. Jin, H. Jin, Z. Du, Y. Zhu, A. Cao, H. Ji and L. J. Wan, *Adv Mater*, 2018, **30**, e1800884-1800890.
4. L. You, S. Ju, J. Liu, G. Xia, Z. Guo and X. Yu, *J Energy Chem*, 2022, **65**, 439-447.